

Real-Time In Vivo Green Fluorescent Protein Imaging of a Murine Leishmaniasis Model as a New Tool for *Leishmania* Vaccine and Drug Discovery[∇]

Sanjay R. Mehta,¹ Robert Huang,¹ Meng Yang,² Xing-Quan Zhang,¹ Bala Kolli,³ Kwang-Poo Chang,³ Robert M. Hoffman,^{2,4} Yasuyuki Goto,⁵ Roberto Badaro,^{1,6} and Robert T. Schooley^{1*}

Department of Medicine, University of California, San Diego, San Diego, California¹; AntiCancer Inc., San Diego, California²; Department of Microbiology/Immunology, Rosalind Franklin University/Chicago Medical School, Chicago, Illinois³; Department of Surgery, University of California, San Diego, San Diego, California⁴; Infectious Diseases Research Institute, Seattle, Washington⁵; and Federal University of Bahia, Salvador, Brazil⁶

Received 28 July 2008/Accepted 13 October 2008

***Leishmania* species are obligate intracellular protozoan parasites that cause a broad spectrum of clinical diseases in mammalian hosts. The most frequently used approach to quantify parasites in murine model systems is based on thickness measurements of the footpad or ear after experimental infection. To overcome the limitations of this method, we used a *Leishmania* mutant episomally transfected with enhanced green fluorescent protein, enabling in vivo real-time whole-body fluorescence imaging, to follow the progression of *Leishmania* infection in parasitized tissues. Fluorescence correlated with the number of *Leishmania* parasites in the tissue and demonstrated the real-time efficacy of a therapeutic vaccine. This approach provides several substantial advantages over currently available animal model systems for the in vivo study of immunopathogenesis, prevention, and therapy of leishmaniasis. These include improvements in sensitivity and the ability to acquire real-time data on progression and spread of the infection.**

Leishmania parasites have been known human pathogens for centuries and continue to cause significant morbidity and mortality. Over 350 million people are at risk of *Leishmania* infection, and at least 500,000 new cases with severe morbidity are reported yearly (24). Additionally, *Leishmania* spp. are emerging as important opportunistic pathogens in persons coinfecting with human immunodeficiency virus type 1. Therapeutic options for managing leishmaniasis are limited, and many have significant toxicity. Rapid advances in computational proteomics and synthetic chemistry coupled with new high-throughput screening technologies raise the likelihood that within a few years many new compounds could be ready for testing in animal model systems. Furthermore, several groups around the world are exploring novel and previously characterized molecules for use as vaccines against leishmaniasis (6, 14).

Murine models of leishmaniasis have been extensively used to study the pathogenesis of the disease and to test novel therapeutic and immunoprophylactic agents (18). *Leishmania* infection of BALB/c mice often results in uncontrolled growth of the parasite at the primary site of the infection followed by progressive dissemination through the lymph nodes into the reticuloendothelial system (22). These mice are susceptible to infection by various *Leishmania* species, including *L. major* and *L. amazonensis* as presented here (7, 17). The standard method for following infection in this in vivo model is based on estimation of parasite loads by labor-intensive microscopic enumeration of sacrificed animals or caliper-based measurements

of the size or thickness of lesions that have developed at the site of infection, such as the footpad, ear dermis, or tail base (7, 22).

Optical techniques are now available for whole-body imaging of small animals using luciferase and green fluorescent protein (GFP) (10, 11, 25, 26). Bioluminescent *Leishmania* expressing luciferase has recently been used for monitoring infection in mouse macrophages, as well as in living mice (15). Several of us have pioneered in vivo imaging with GFP to visualize tumors and infectious agents such as *Salmonella enterica* serovar Typhimurium in live mice (10, 26, 27). Recently, in an experimental model of malaria, imaging of *Plasmodium berghei* transfected with GFP demonstrated the dynamics of infection directly in live mice (1). GFP-transfected *Leishmania* parasites have been used to screen for antileishmanial activity in cell cultures by flow cytometry and microtiter plate assays (5, 8, 12, 23). Herein we describe the use of episomally GFP-transfected *Leishmania* in a whole-body imaging system to follow the dynamics of infection.

MATERIALS AND METHODS

This study was conducted under University of California, San Diego (UCSD), animal protocol S05322 under the auspices of the UCSD Institutional Animal Care and Use Committee.

Transfected parasites. Enhanced GFP gene (*egfp*) transfectants of *L. amazonensis* (LV78, clone 12-1) were prepared as described. Briefly, *egfp* was cloned into the BamHI site of p6.5, a *Leishmania*-specific vector, for expansion in *Escherichia coli*. The constructs obtained were used to transfect stationary-phase promastigotes by electroporation (9, 13). Electroporated cells were then selected for resistance to tunicamycin at 10 μ g/ml. Stable transfectants were passaged continuously under these selective conditions in vitro in medium M199 buffered to pH 7.4 with 50 mM HEPES and fortified with 10% heat-inactivated fetal bovine serum.

In vitro culture system. *egfp*-transfected *Leishmania amazonensis* parasites harvested from mouse footpads were expanded in standard nonventilated tissue

* Corresponding author. Mailing address: Stein Clinical Research Bldg. 402A, 9500 Gilman Drive Box 0711, La Jolla, CA 92093. Phone: (858) 822-4092. Fax: (858) 822-5362. E-mail: rschooley@ucsd.edu.

[∇] Published ahead of print on 22 October 2008.

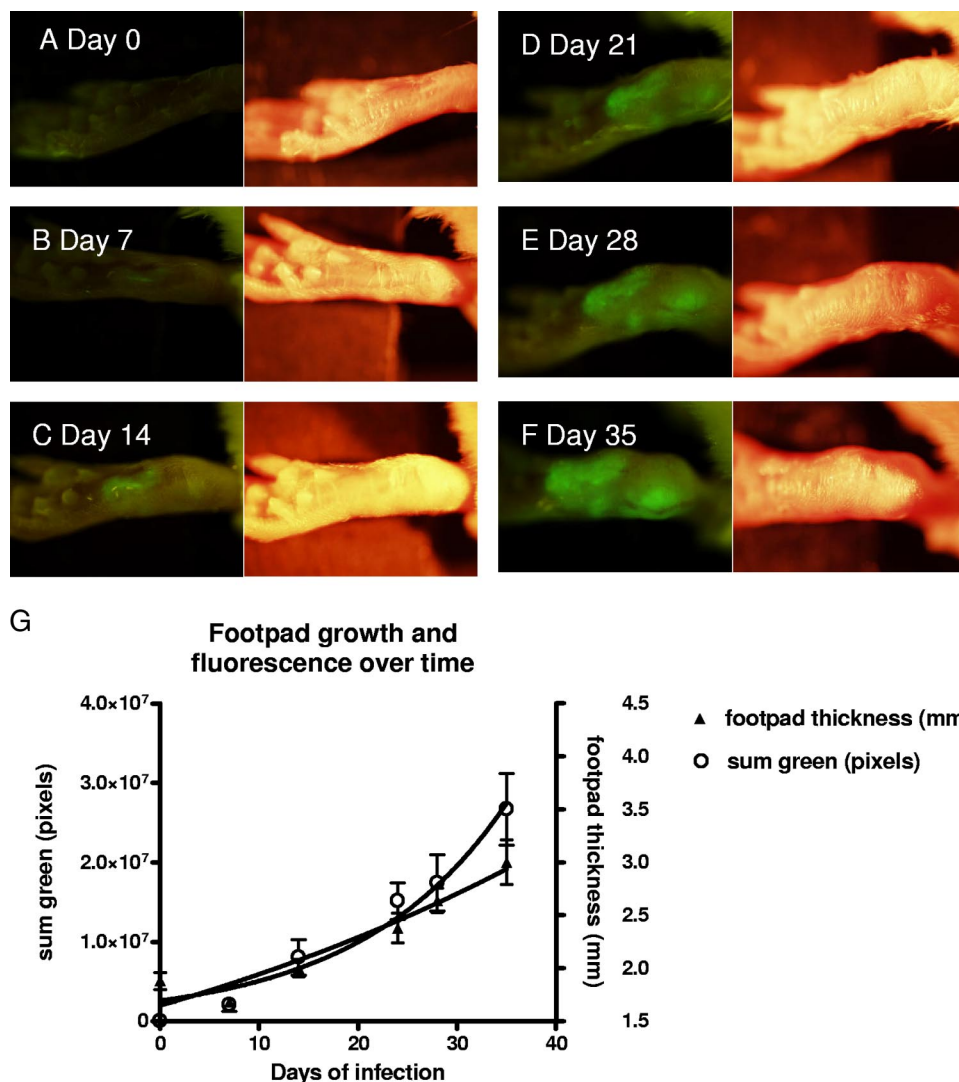


FIG. 1. Photographs of a mouse footpad over time after inoculation with 10^7 *egfp*-transfected *L. amazonensis* promastigotes. (A to F) On each pair of photographs, the left image was taken using the fluorescence imaging system, while the right image was taken using normal bright-field imaging. The images were taken at 7-day intervals, as indicated in the figure, with the day 0 photograph taken just prior to inoculation. Photographs were taken using the OV-100 imaging system (Olympus, Tokyo, Japan). Five mice were used in this experiment, and one representative mouse was chosen for all of the photographs. (G) Graph of the mean footpad measurement in mm (right axis) with standard error over the course of the *Leishmania* infection (solid triangles). On the same graph, the mean of the sum green pixel count (open circles) with standard error from images taken at serial time points is plotted as well (left axis). GFP fluorescence, indicating infection, was visualized when the first set of images was taken at day 7. A significant difference in the mean measurements between day 0 and each time point was not reached until day 24 ($P = 0.011$).

culture flasks in M199 medium supplemented with 20% heat-inactivated fetal calf serum, 1 mg hemin (Sigma H-1652), 0.25 ml of 0.1% biotin in 95% ethanol (Sigma B-4639), 50 mM HEPES (Sigma H-1552), 100 U/ml penicillin, and 100 μ g/ml streptomycin (Gibco BRL 25030-081). Cultures were maintained at 25°C, and the parasites were passaged by 1:9 dilution weekly. The transfectants were grown for one cycle without selective pressure before inoculation to avoid the introduction of cytotoxic tunicamycin into the recipient mice.

In vivo (murine) model of infection. The right hind footpads of female BALB/c mice aged 8 to 12 weeks were subcutaneously injected each with 10^7 *egfp*-transfected late-stationary-phase *L. amazonensis* promastigotes suspended in 100 μ l of phosphate-buffered saline (PBS), using a 26-gauge needle. GFP fluorescence was demonstrated within mouse footpads up to 3 months after inoculation (unpublished observations).

Imaging. The footpads of the mice were imaged weekly, beginning at day 0, with the Olympus OV-100 small-animal imaging system as described below (25). Mice were treated with a depilatory substance (Nair) to remove hair from their legs and feet to reduce background autofluorescence. They were then tempo-

rarily anesthetized with xylazine-ketamine-acepromazine solution given intraperitoneally and then imaged on days 0, 7, 14, 24, 28, and 35 after inoculation. Photographs were taken after exposure for 1.5 s with a focal length of 40.7 mm. Pixel counting and measurement of the lesions were performed using Olympus software. Measurements were reported as "sum green," a quantitative measurement defined as the number of green pixels in a given area multiplied by the average intensity of each pixel.

Presence of *Leishmania* within tissue. Mice were sacrificed for collection of samples from infected footpads, from which frozen sections 5 μ m in thickness were prepared. Fluorescence pictures were taken using a Nikon E600 microscope prior to fixation. Additional sections were cut and fixed with cold acetone and stained with F4 80 (rat anti-mouse macrophage antibody subsequently biotinylated and labeled with phycoerythrin) and DAPI (4',6-diamidino-2-phenylindole), to demonstrate colocalization.

Immunotherapy with Leish 111f + MPL-SE vaccine. BALB/c mice divided into groups of five were inoculated in the right footpad with 10^7 *egfp*-transfected *L. amazonensis* promastigotes. On days 7, 14, and 24, the mice in the control arm

received subcutaneous injections of 25 μ l of PBS into the footpad. The mice in the vaccine group received 100 μ l of the Leish 111f + MPL-SE vaccine on days 7, 14, and 24, of which 30 μ l was injected subcutaneously into the inoculated footpad and 70 μ l was injected subcutaneously into the right flank of the mouse. Imaging was performed weekly as described above, and the mice were euthanized on day 41 of the experiment.

Statistical analysis. Prism 4.0 (Graphpad Software, Carlsbad, CA) was used to create charts and best curve fits using a nonlinear regression exponential growth model. Intergroup comparisons were analyzed by the unpaired Students *t* test using the same statistical package.

RESULTS

In order to determine whether we could detect GFP-labeled transfectants *in vivo* using whole-body imaging, we subcutaneously injected 10^7 GFP transfectants into the hind footpads of BALB/c mice (9, 13). The mice were examined weekly for 5 weeks with the Olympus OV-100 (Olympus, Tokyo, Japan) fluorescence small-animal imaging system (25). GFP fluorescence, which was initially localized to the site of the inoculation, subsequently spread progressively to a wider area over the course of the next 5 weeks (Fig. 1). Progression of the lesion with time of infection was easily and precisely delineated by measuring pixel counts of the fluorescent images using Olympus OV-100 imaging software. Measurements toward the end of the 5-week period showed increasing thickness of the footpads. However, the first several measurements for each of the mice were variable and did not demonstrate a clear trend of increasing thickness.

In Fig. 2, BALB/c mice were inoculated with increasing numbers of *egfp*-transfected *L. amazonensis* parasites. The time of initial detection using the *in vivo* imaging method is plotted for each of the inoculums placed. By our estimation, until there was a 40% increase in footpad size, the variability in the measurements precluded any determination of whether or not true infection is present. The relationship of footpad thickness with fluorescence shows that it took 12 more days after initial detection by imaging (Fig. 1G) before we felt that we could adequately deduce infection using the traditional caliper-based method.

The fluorescence visualized by whole-body imaging was confirmed to be *Leishmania* by direct fluorescence microscopy of infected tissues. *Leishmania* amastigotes were seen as fluorescent bodies in 5- μ m cryo-sections (Fig. 3a). Persistence of fluorescence 5 weeks after inoculation was demonstrated in individual parasites in Fig. 3b to d. Immunostaining of the preparations demonstrated colocalization of the GFP with macrophages verifying that the *Leishmania* amastigotes were intracellular (not shown).

GFP fluorescence intensity was reflective of parasite burden in the footpads, as demonstrated by the footpads of seven mice that were inoculated with increasing concentrations of *egfp*-transfected *Leishmania amazonensis* parasites and then imaged. We found that the sum green pixel counts from the imaging studies were proportional to the number of the transfectants injected into each footpad (Fig. 4), suggesting that imaging could be used as a semiquantitative correlate of the number of parasites *in vivo*.

We then applied this approach to the evaluation of an experimental immunotherapy against leishmaniasis that had previously been shown to be clinically effective on a compassionate use basis. Recently, the use of the recombinant polyprotein

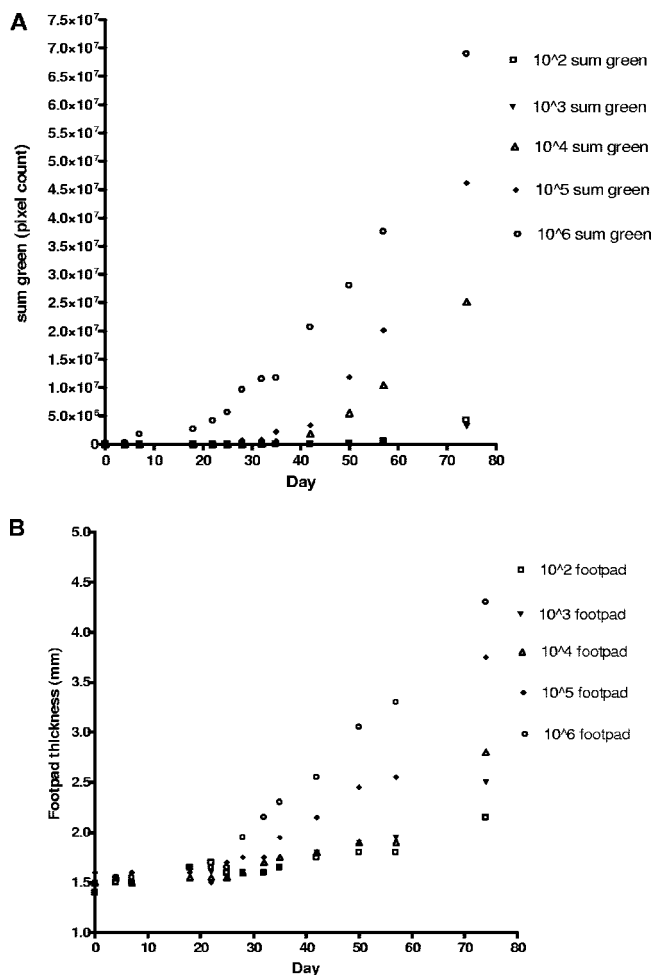


FIG. 2. Mouse footpads were inoculated with increasing numbers of *egfp*-transfected *Leishmania amazonensis* parasites from 10^2 to 10^6 promastigotes. Mice were followed over time, and footpad measurements and fluorescence imaging were done at regular intervals. The times of first detection of fluorescence for each inoculation were as follows: 10^6 , 4 days; 10^5 , 18 days; 10^4 , 32 days; 10^3 , 42 days; and 10^2 , 42 days. (A) Graph of sum green pixel count in the fluorescence image at each time point for each inoculation dose. (B) Graph of footpad thickness at each time point for each inoculation dose. Data from two mice were averaged for each data point.

Leish 111f + MPL-SE, comprised of the leishmanial antigens in equal parts designated as TSA (heat shock protein 83), LmSTI1 (stress-inducible protein 1), and LeIF (*Leishmania* elongation initiation factor), along with MPL-SE as an immunological adjuvant, demonstrated efficacy in the treatment of refractory mucosal leishmaniasis (2). We inoculated two groups of five mice each with 10^7 GFP-transfected promastigotes from culture into mouse footpads. Infection became visible by tissue imaging for GFP fluorescence 1 week after inoculation. Swelling of inoculated footpads was not demonstrable using traditional caliper-based methods until almost 3 weeks after the inoculation. We began weekly immunotherapeutic treatments 1 week after inoculation with the Leish 111f + MPL-SE vaccine and PBS alone for the control group. Progression of the infection was monitored by real-time imaging for GFP intensity. Immunotherapy of the infected mice for 3

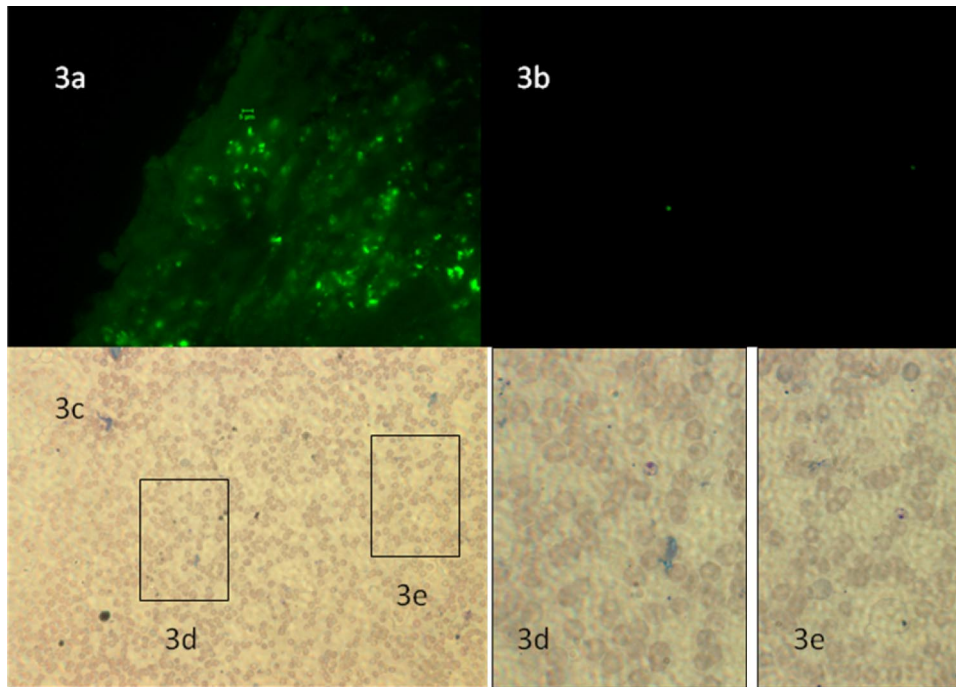


FIG. 3. (a) Fluorescence micrograph of a tissue section taken 42 days after inoculation with a Nikon E600 at $\times 1,000$. The GFP-containing amastigote bodies are seen as the scattered green dots in the tissue section. (b) Fluorescence micrograph taken at $\times 400$ of a touch preparation of a mouse footpad infected for 5 weeks after inoculation with GFP-transfected *L. amazonensis*. Panel c shows the same touch preparation at the corresponding area of the slide taken at $\times 400$ stained with Hema 3. (d) Magnification at $\times 1,000$ of inset 3d, which demonstrates the presence of an *L. amazonensis* amastigote stained with Hema 3 that also corresponds to the fluorescent parasite in the bottom left corner of Fig. 3b. (e) Magnification at $\times 1,000$ of inset 3e, which demonstrates the presence of an *L. amazonensis* amastigote stained with Diff-Quick that is again expressing GFP based on the fluorescence micrograph shown in panel b.

weeks with the vaccine significantly suppressed the infection when compared with the control. This was shown much sooner using measurement of GFP intensity when compared to footpad measurements (Fig. 5). The results obtained are consistent with recent work by Calvopina et al., who investigated the therapeutic effects of soluble *Leishmania* amastigote antigens in combination with the synthetic lipid A analog ONO-4007 as

an adjuvant in a murine model of cutaneous leishmaniasis as assessed by footpad swelling (4).

DISCUSSION

Our work describes the application of whole-body fluorescent imaging in the murine model for the study of leishmani-

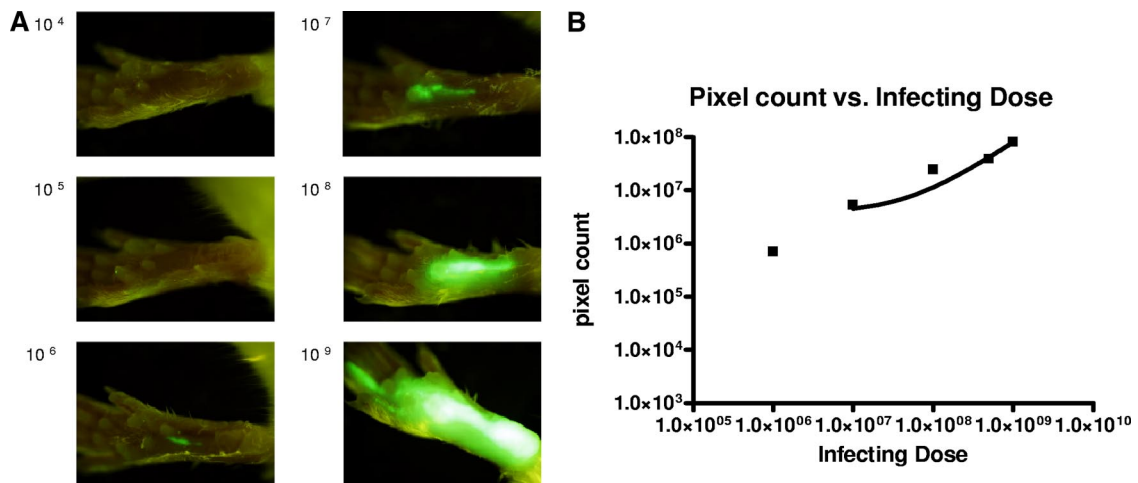


FIG. 4. (A) Images taken 2 h after inoculation with increasing numbers of *egfp*-transfected *L. amazonensis* parasites. (B) Graph of pixel counts of green fluorescence against the number of *Leishmania* parasites inoculated, showing the relationship between infecting dose and pixel count ($r = 0.9798$ by the Pearson method). The solid line represents the best-fit curve using linear regression.

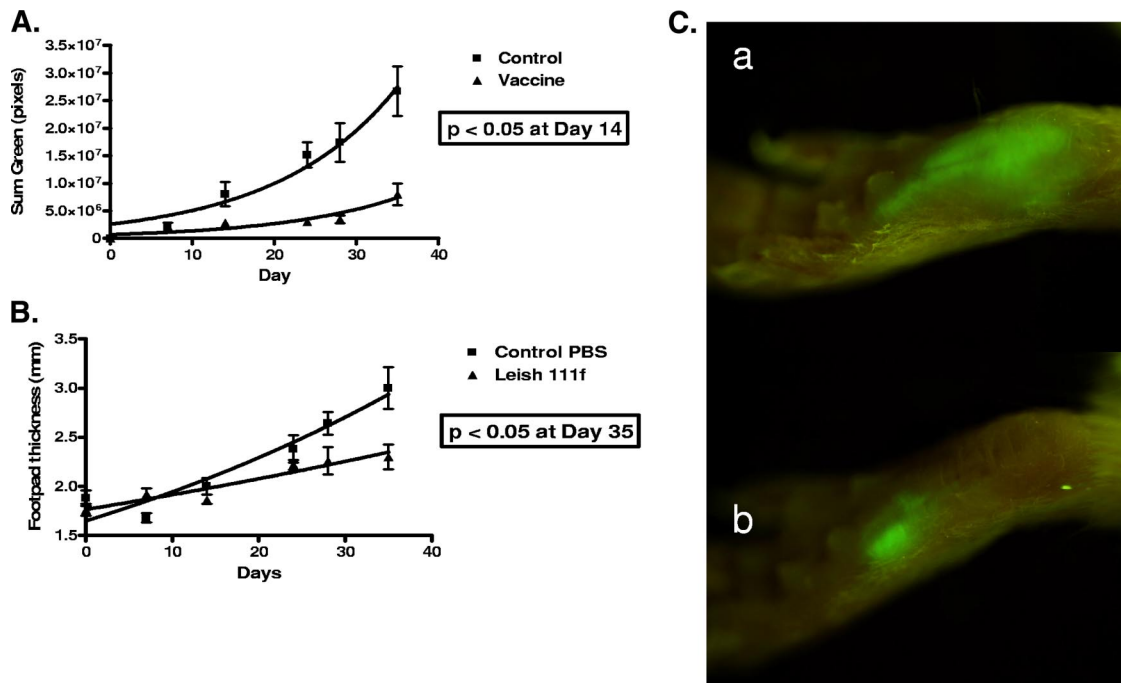


FIG. 5. Immunotherapeutic suppression of *Leishmania* growth with Leish 111f + MPL-SE. (A) Graph of the sum green pixel count from mice inoculated with 10^7 *egfp*-transfected *L. amazonensis* promastigotes versus time. Five mice in each group were imaged weekly. The mice in the control group received 25 μ l of PBS injected into the inoculated footpad at days 7, 14, and 24. The mice in the vaccine group received 100 μ l of the Leish 111f + MPL-SE vaccine divided between the right flank and the inoculated footpad at days 7, 14, and 24. Solid lines represent best-fit curves using a nonlinear regression exponential growth equation. (B) Graph of the footpad measurements of the mice from the same experiment. The measurements of footpad thickness and GFP at each time point were compared between the control group and the treatment group and analyzed using the unpaired Student's *t* test. The difference in footpad measurements between groups did not reach statistical significance ($P < 0.05$) until day 35, while the difference in GFP signals between groups was statistically significant at day 14. (C) Representative photographs of a footpad from the control group, a, and the vaccinated group, b, at 24 days.

asis. This new method using GFP-transfected *Leishmania* to induce murine cutaneous leishmaniasis is a novel dynamic immunopathogenic model that allows visualization and correlation of fluorescence intensity with parasite burden. Our fluorescence measurements correlate with parasite burden and are more sensitive and precise than the standard caliper-based method of following *Leishmania* infection in vivo. Although the sensitivity of detection was 10^6 microorganisms in this model, previous experiments established that at this level of microorganism burden, the size of the lesion was undetectable by caliper measurements but clearly visible by fluorescent imaging.

Luciferase has also been used as a reporter for in vivo imaging of *Leishmania* and *Leishmania* parasites stably transfected with luciferase have been detected in vivo using an ear model 1 day after 10^5 organisms were inoculated (15). However, there are several limitations to this approach. Luciferase requires the substrate luciferin, which must be administered intravenously or intraperitoneally each time imaging is performed. The luminescence produced is unstable and dependent upon the metabolic activity of cells transfected with luciferase, which can vary depending upon where in the lesion parasites are located, time of day, and other factors. Finally, fluorescence imaging allows for actual imaging, while quantification with luminescence requires photon counting, and can only generate a pseudoimage. This is important when studying

tissue harvested from an infected animal, as parasites can be visualized individually.

Fluorescent imaging offers several advantages. In vitro systems have demonstrated that fluorescence measurements are proportional to the number of *Leishmania* amastigotes present (20). Episomal transfection was chosen because it provided significantly higher levels of fluorescence. Roy et al. demonstrated successful chromosomal integration of the luciferase gene into the ribosomal promoter region of *L. major* and *L. donovani*. In their work, they noted that these parasites were almost $2 \log_{10}$ less luminescent than the episomal transfectants (21). Recent work has shown that *Leishmania* parasites constitutively express their entire genome and that gene expression modification occurs posttranscriptionally (16). Because of this, the expression of a gene integrated into the *Leishmania* chromosome will be dependent on many factors. *Leishmania* transfectants retain episomal plasmids in the absence of selective pressure for prolonged periods (23). GFP expression stability in vivo has been well demonstrated previously in tumor growth, metastasis, and angiogenesis models (10). In hamster ovary cells, episomal expression of GFP has been shown to remain stable even after 24 days in the absence of selective pressure (19). Furthermore, in our system we followed mice infected with 100 GFP-transfected *Leishmania* parasites for greater than 8 weeks and despite the lack of selective pressure in vivo, fluorescence was visualized after 70 days.

Previous studies have classically described footpad measurements using calipers to estimate the severity of infection by measuring the thickness of the footpad, observing for signs of ulceration, and monitoring other clinical parameters that do not necessarily represent the burden of infection but may reflect inflammation (3, 6). In our model, we directly measure parasite burden using the GFP fluorescence expressed by the parasites. Our fluorescence imaging system gives a precise two-dimensional image of the extent of infection, independent of the inflammatory response. This measurement method has been well established in the measurement of fluorescing tumor lesions in vivo, and we now describe its use in murine cutaneous leishmaniasis (26). The tissue penetration of the GFP fluorescence and our imaging software allow us to make an approximation of the integration of total fluorescence through multiple planes. Therefore, although we are using single-plane imaging, we can determine an approximation of the total volume of infection. The future may yield improvements in small-animal imaging resolution through tomography or volumetric imaging using Z-series, a method of imaging that allows a more three-dimensional view of the image by taking images in serial depths similar to tomography.

The sensitivity of this technique makes it extremely useful for monitoring *Leishmania* in vivo. The intensity of GFP fluorescence and the sensitivity of our detection system gave us a limit of detection of $\sim 10^6$ organisms per footpad by real-time in vivo imaging. From our experiments using an inoculum of 10^6 promastigotes, we have found that detection of infection by whole-body imaging precedes that demonstrated by Vernier calipers by nearly 2 weeks. These advantages outweigh some of the inherent problems with the system: i.e., variability in the GFP fluorescence among individual parasites and diminishing plasmid copy number and fluorescence with the duration of time in vivo in the absence of selective pressure.

In conclusion, the application of GFP fluorescence for in vivo imaging provides a novel murine model of cutaneous leishmaniasis that allows for the evaluation of the dynamics of ongoing infection in the same mice. In comparison with the classical footpad caliper measurements, we avoid the disadvantages of (i) substantial variability associated with the current and routine caliper-based methods that require the use of large numbers of animals to obtain statistically reliable data; (ii) measurement in a single vector to quantify a three-dimensional infection; and (iii) difficulty in differentiating the extent of infection from local immune response. Our model is qualitative and semiquantitative, markedly more sensitive and precise than the standard caliper-based method of following infection, and reduces experimental variation by allowing investigators to follow the same mouse through the course of an experiment, rather than sacrificing multiple groups of mice at serial time points. This powerful noninvasive whole-body imaging tool creates new opportunities for studying immunopathogenesis in murine leishmaniasis and for the evaluation of new prophylactic and therapeutic agents and represents a significant refinement over previous animal models.

ACKNOWLEDGMENTS

Support for the development of the model was also provided by the UCSD Center for AIDS Research and by NIAID Institutional Post-

doctoral Training grant 5T32AI007036. K.P.C. and B.K. are supported by NIH AI-20486 and AI-68835.

We thank Steven Baird for assistance with frozen tissue sections; Keith Jenne for assistance with photography and animal care; and finally Jim Feramisco, Kersi Pestonjamas, and the UCSD Cancer Center Histology Core for assistance with immunofluorescence imaging.

R.M.H. is president of AntiCancer, Inc. Y.G. is an employee of the Infectious Disease Research Institute. All other authors report no financial conflicts of interest.

REFERENCES

1. Amino, R., S. Thiberge, B. Martin, S. Celli, S. Shorte, F. Frischknecht, and R. Menard. 2006. Quantitative imaging of *Plasmodium* transmission from mosquito to mammal. *Nat. Med.* **12**:220–224.
2. Badaro, R., I. Lobo, A. Munos, E. M. Netto, F. Modabber, A. Campos-Neto, R. N. Coler, and S. G. Reed. 2006. Immunotherapy for drug-refractory mucosal leishmaniasis. *J. Infect. Dis.* **194**:1151–1159.
3. Calvopina, M., P. A. Barroso, J. D. Marco, M. Korenaga, P. J. Cooper, S. Nonaka, and Y. Hashiguchi. 2006. Efficacy of vaccination with a combination of *Leishmania* amastigote antigens and the lipid A-analogue ONO-4007 for immunoprophylaxis and immunotherapy against *Leishmania amazonensis* infection in a murine model of New World cutaneous leishmaniasis. *Vaccine* **24**:5645–5652.
4. Calvopina, M., H. Uezato, E. A. Gomez, M. Korenaga, S. Nonaka, and Y. Hashiguchi. 2006. Leishmaniasis recidiva cutis due to *Leishmania* (*Viannia*) *panamensis* in subtropical Ecuador: isoenzymatic characterization. *Int. J. Dermatol.* **45**:116–120.
5. Chan, M. M., J. C. Bulinski, K. P. Chang, and D. Fong. 2003. A microplate assay for *Leishmania amazonensis* promastigotes expressing multimeric green fluorescent protein. *Parasitol. Res.* **89**:266–271.
6. Coler, R. N., Y. A. Skeiky, K. Bernards, K. Greeson, D. Carter, C. D. Cornellison, F. Modabber, A. Campos-Neto, and S. G. Reed. 2002. Immunization with a polyprotein vaccine consisting of the T-cell antigens thiol-specific antioxidant, *Leishmania major* stress-inducible protein 1, and *Leishmania* elongation initiation factor protects against leishmaniasis. *Infect. Immun.* **70**:4215–4225.
7. Courret, N., T. Lang, G. Milon, and J. C. Antoine. 2003. Intradermal inoculations of low doses of *Leishmania major* and *Leishmania amazonensis* metacyclic promastigotes induce different immunoparasitic processes and status of protection in BALB/c mice. *Int. J. Parasitol.* **33**:1373–1383.
8. Dube, A., N. Singh, S. Sundar, and N. Singh. 2005. Refractoriness to the treatment of sodium stibogluconate in Indian kala-azar field isolates persist in in vitro and in vivo experimental models. *Parasitol. Res.* **96**:216–223.
9. Dutta, S., D. Ray, B. K. Kolli, and K.-P. Chang. 2005. Photodynamic sensitization of *Leishmania amazonensis* in both extracellular and intracellular stages with aluminum phthalocyanine chloride for photolysis in vitro. *Antimicrob. Agents Chemother.* **49**:4474–4484.
10. Hoffman, R. M. 2005. The multiple uses of fluorescent proteins to visualize cancer in vivo. *Nat. Rev. Cancer* **5**:796–806.
11. Hoffman, R. M., and M. Yang. 2005. Dual-color, whole-body imaging in mice. *Nat. Biotechnol.* **23**:790.
12. Kamau, S. W., F. Grimm, and A. B. Hehl. 2001. Expression of green fluorescent protein as a marker for effects of antileishmanial compounds in vitro. *Antimicrob. Agents Chemother.* **45**:3654–3656.
13. Kawazu, S., H. G. Lu, and K. P. Chang. 1997. Stage-independent splicing of transcripts two heterogeneous neighboring genes in *Leishmania amazonensis*. *Gene* **196**:49–59.
14. Khamesipour, A., S. Rafati, N. Davoudi, F. Maboudi, and F. Modabber. 2006. Leishmaniasis vaccine candidates for development: a global overview. *Indian J. Med. Res.* **123**:423–438.
15. Lang, T., S. Goyard, M. Lebastard, and G. Milon. 2005. Bioluminescent *Leishmania* expressing luciferase for rapid and high throughput screening of drugs acting on amastigote-harboring macrophages and for quantitative real-time monitoring of parasitism features in living mice. *Cell. Microbiol.* **7**:383–392.
16. Leifso, K., G. Cohen-Freue, N. Dogra, A. Murray, and W. R. McMaster. 2007. Genomic and proteomic expression analysis of *Leishmania* promastigote and amastigote life stages: the *Leishmania* genome is constitutively expressed. *Mol. Biochem. Parasitol.* **152**:35–46.
17. Louis, J., A. Gummy, H. Voigt, M. Rocken, and P. Launois. 2002. Experimental cutaneous Leishmaniasis: a powerful model to study in vivo the mechanisms underlying genetic differences in Th subset differentiation. *Eur. J. Dermatol.* **12**:316–318.
18. Murray, H. W., E. B. Brooks, J. L. DeVecchio, and F. P. Heinzel. 2003. Immunoenhancement combined with amphotericin B as treatment for experimental visceral leishmaniasis. *Antimicrob. Agents Chemother.* **47**:2513–2517.
19. Naumov, G. N., S. M. Wilson, I. C. MacDonald, E. E. Schmidt, V. L. Morris, A. C. Groom, R. M. Hoffman, and A. F. Chambers. 1999. Cellular expression of green fluorescent protein, coupled with high-resolution in

- vivo videomicroscopy, to monitor steps in tumor metastasis. *J. Cell Sci.* **112**:1835–1842.
20. Okuno, T., Y. Goto, Y. Matsumoto, H. Otsuka, and Y. Matsumoto. 2003. Applications of recombinant *Leishmania amazonensis* expressing egfp or the beta-galactosidase gene for drug screening and histopathological analysis. *Exp. Anim.* **52**:109–118.
 21. Roy, G., C. Dumas, D. Sereno, Y. Wu, A. K. Singh, M. J. Tremblay, M. Ouellette, M. Olivier, and B. Papadopolou. 2000. Episomal and stable expression of the luciferase reporter gene for quantifying *Leishmania* spp. infections in macrophages and in animal models. *Mol. Biochem. Parasitol.* **110**:195–206.
 22. Sacks, D., and C. Anderson. 2004. Re-examination of the immunosuppressive mechanisms mediating non-cure of *Leishmania* infection in mice. *Immunol. Rev.* **201**:225–238.
 23. Singh, N., and A. Dube. 2004. Short report: fluorescent *Leishmania*: application to anti-leishmanial drug testing. *Am. J. Trop. Med. Hyg.* **71**:400–402.
 24. World Health Organization. 2002. The leishmaniasis and *Leishmania*/HIV co-infections. World Health Organization, Geneva, Switzerland.
 25. Yamauchi, K., M. Yang, P. Jiang, M. Xu, N. Yamamoto, H. Tsuchiya, K. Tomita, A. R. Moossa, M. Bouvet, and R. M. Hoffman. 2006. Development of real-time subcellular dynamic multicolor imaging of cancer cell trafficking in live mice with a variable-magnification whole-mouse imaging system. *Cancer Res.* **66**:4208–4214.
 26. Yang, M., E. Baranov, P. Jiang, F. X. Sun, X. M. Li, L. Li, S. Hasegawa, M. Bouvet, M. Al-Tuwaijri, T. Chishima, H. Shimada, A. R. Moossa, S. Penman, and R. M. Hoffman. 2000. Whole-body optical imaging of green fluorescent protein-expressing tumors and metastases. *Proc. Natl. Acad. Sci. USA* **97**:1206–1211.
 27. Zhao, M., M. Yang, X. M. Li, P. Jiang, E. Baranov, S. Li, M. Xu, S. Penman, and R. M. Hoffman. 2005. Tumor-targeting bacterial therapy with amino acid auxotrophs of GFP-expressing *Salmonella typhimurium*. *Proc. Natl. Acad. Sci. USA* **102**:755–760.